Accuracy of macroscopic and microscopic pK_a predictions of small molecules evaluated by the SAMPL6 blind prediction challenge

Mehtap Işık (ORCID: 0000-0002-6789-952X)[1,2,*], **Ariën S. Rustenburg (ORCID: 0000-0002-3422-0613)**[1,3], **Andrea Rizzi (ORCID: 0000-0001-7693-2013)**[1,4], **M. R. Gunner**[6], **David L. Mobley (ORCID: 0000-0002-1083-5533)**[5], **John D. Chodera (ORCID: 0000-0003-0542-119X)**[1]

[1]Computational and Systems Biology Program, Sloan Kettering Institute, Memorial Sloan Kettering Cancer Center, New York, NY 10065, United States; [2]Tri-Institutional PhD Program in Chemical Biology, Weill Cornell Graduate School of Medical Sciences, Cornell University, New York, NY 10065, United States; [3]Graduate Program in Physiology, Biophysics, and Systems Biology, Weill Cornell Medical College, New York, NY 10065, United States; [4]Tri-Institutional PhD Program in Computational Biology and Medicine, Weill Cornell Graduate School of Medical Sciences, Cornell University, New York, NY 10065, United States; [5]Department of Pharmaceutical Sciences and Department of Chemistry, University of California, Irvine, Irvine, California 92697, United States; [6]Department of Physics, City College of New York, New York NY 10031

*For correspondence:
mehtap.isik@choderalab.org (MI)

Abstract

Complete abstract.

- number of submissions [1]
- summary of analysis
- difficulties observed

0.1 Keywords

SAMPL · blind prediction challenge · acid dissociation constant · pK_a · small molecule · macroscopic pK_a· microscopic pK_a· macroscopic protonation state · microscopic protonation state

0.2 Abbreviations

SAMPL Statistical Assessment of the Modeling of Proteins and Ligands

pK_a $-\log_{10}$ acid dissociation equilibrium constant

SEM Standard error of the mean

RMSE Root mean squared error

MAE Mean absolute error

τ Kendall's rank correlation coefficient (Tau)

R^2 Coefficient of determination (R-Squared)

1 Introduction

SAMPL (Statistical Assessment of the Modeling of Proteins and Ligands). About SAMPL challenges: Collectively, these challenges have assessed the effects of force field accuracy, solvation models, pKa and tautomer predictions.

During the SAMPL5 challenge, log D predictions experienced difficulties predicting log D values accurately, unless protonation states and tautomers were taken into account.

For this iteration of the SAMPL challenge, we have taken one step back and isolated just the problem of predicting solvent protonation states.

This is the first time a blind pKa prediction challenge has been fielded as part of SAMPL. In this first iteration of the challenge, we aimed to assess the performance of current pKa prediction methods and isolate potential causes of inaccurate pKa estimates, with the aim of determining how pKa prediction inaccuracies might impact predicted affinities for drug-like molecules. For example, for both logD and binding affinity predictions, any error in predicting the free energy of accessing a minor protonation state in solution that becomes dominant in the complex will directly add to the error in the predicted transfer or binding free energy.

Challenge goal: determining how pKa prediction inaccuracies might impact predicted affinities for drug-like molecules. For example, for both logD and binding affinity predictions, any error in predicting the free energy of accessing a minor protonation state in solution that becomes dominant in the complex will directly add to the error in the predicted transfer or binding free energy.

Reason for blind pKa challenge: - Impact on binding affinity predictions - Impact on logD predictions (SAMPL6) - Drug-like molecules are especially challenging.

Protonation state effects were a dominant accuracy-limiting factor for logD from SAMPL5, and should also be accuracy-limiting in binding free energy predictions. Errors is pK_a predictions can cause modeling the wrong charge, protonation and tautomerization states which affect hydrogen bonding opportunities and overall dipole moment of the ligand.

Experimental macroscopic pKa values were measured using a UV-metric assay performed using a Sirius T3 [cite exp. paper] supported by Merck, MRL, Rahway NJ.

Communicate concepts behind challenge design and why we made specific choices: Explain why we have types I, II, III Explain why we preenumerated microstates

Participants had the option to submit predictions in one of 3 categories: Microscopic pKa values (type I), microscopic state populations (type II), or macroscopic pKa values (type III).

The comparison between macroscopic and microscopic pKa values is not always a straightforward one.

Overview of available pKa prediction methods and methods that participated in SAMPL6. [Reminder to cite all papers here.]

Challenge path: predict pKas, give people pKas to predict logDs on same molecules, then predict for new set of compounds logDs without provided pKas.
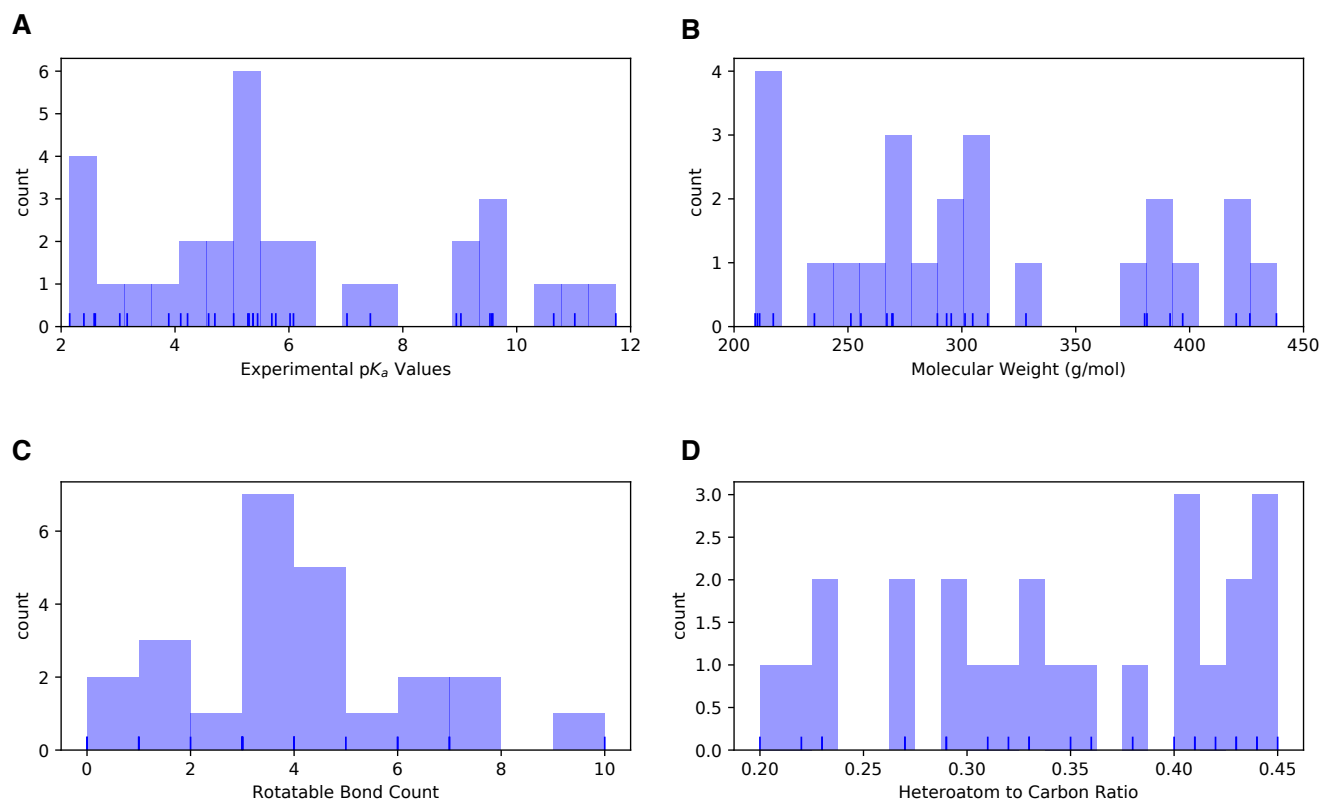
Figure 1. Distribution of molecular properties of 24 compounds in SAMPL6 pK_a Challenge. A Histogram of spectrophotometric pK_a measurements collected with Sirius T3 [1]. Overlayed carpet plot indicates the actual values. Five compounds have multiple measured pK_as in the range of 2-12. **B** Histogram of molecular weights of compounds in SAMPL6 set. Molecular weights were calculated by neglecting counter ions. **C** Histogram of the number of non-terminal rotatable bonds in each molecule. **D** The histogram of the ratio of heteroatom (non-carbon heavy atom) count to the number of carbon atoms.

78

> Explain potential benefits of these challenge

79 Improving computational methods...

1.1 Motivation for a blind pKa challenge

81 why we are doing a pKa challenge and connect to past and previous challenge?

82 SAMPL (Statistical Assessment of the Modeling of Proteins and Ligands). About SAMPL challenges: Collectively, these chal-
83 lenges have assessed the effects of force field accuracy, solvation models, pKa and tautomer predictions.

84 During the SAMPL5 challenge, log D predictions experienced difficulties predicting log D values accurately, unless protonation
85 states and tautomers were taken into account.

86 For this iteration of the SAMPL challenge, we have taken one step back and isolated just the problem of predicting solvent
87 protonation states.

88 This is the first time a blind pKa prediction challenge has been fielded as part of SAMPL. In this first iteration of the challenge,
89 we aimed to assess the performance of current pKa prediction methods and isolate potential causes of inaccurate pKa estimates,
90 with the aim of determining how pKa prediction inaccuracies might impact predicted affinities for drug-like molecules. For
91 example, for both logD and binding affinity predictions, any error in predicting the free energy of accessing a minor protonation
92 state in solution that becomes dominant in the complex will directly add to the error in the predicted transfer or binding free
93 energy.

94 Challenge goal: determining how pKa prediction inaccuracies might impact predicted affinities for drug-like molecules. For
95 example, for both logD and binding affinity predictions, any error in predicting the free energy of accessing a minor protonation
96 state in solution that becomes dominant in the complex will directly add to the error in the predicted transfer or binding free
97 energy.

98 Reason for blind pKa challenge: 1. Impact on binding affinity predictions 2. Impact on logD predictions (SAMPL6) 3. Drug-like
99 molecules are especially challenging.

100 Future challenge direction Challenge path: predict pKas, give people pKas to predict logDs on same molecules, then predict
101 for new set of compounds logDs without provided pKas. Potantial benefits of these challenges: 1. Improving computational
102 methods 2. Detecting hidden contributors to error

1.2 Approaches to predict pKas

104 Overview of kinds of pKa prediction methods available (ML, QM, empirical methods ...

2 Methods

2.1 Structure and logistics of the SAMPL6 pKa prediction challenge

107

> Describe the structure of SAMPL6 pKa challenge

108 Experimental macroscopic pKa values were measured using a UV-metric assay performed using a Sirius T3 [cite exp. paper
109] supported by Merck, MRL, Rahway NJ.

110 Communicate concepts behind challenge design and why we made specific choices: 1. Explain why we have types I, II, III 2.
111 Explain why we pre-enumerated microstates

112 Participants had the option to submit predictions in one of 3 categories: Microscopic pKa values (type I), microscopic state
113 populations (type II), or macroscopic pKa values (type III).

114 The comparison between macroscopic and microscopic pKa values is not always a straightforward one.

115 - When instructions and input files were made available

116 - Challenge dates

117 - Input files

118 - What to predict? Three type of submissions.

119 - Multiple submissions allowed

120 - Predicting the pKa values of the whole set wasn't a requirement.

121 - 2nd D3R/SAMPL Workshop took place in La Jolla, San Diego on Feb 22-23, 2018.

122 Referece Figure **??**. Drug-like molecules are often larger and more complex than the ones used in this study.

2.2 Enumeration of requested prediction microscopic protonation states

124 1. OpenEye (filter out resonance structures), Epik

125   2. Participant supplied structures

126   Microstate pairs: Only +/-1 charge change transitions are allowed. List of allowed transitions. +2 transitions are not consid-

127 ered.

2.3 Evaluation approaches

2.3.1 Statistical metrics for submission performance

130 - Root mean squared error (RMSE)

131   - Mean absolute error (MAE)

132   - Mean Error (ME)

133   - Square of Pearson Correlation Coefficient (R^2)

134   - Slope of prediction vs. experimental value linear fit

135   Uncertainty in each performance statistic was calculated by bootstapping (10,000) to estimate 95% confidence intervals.

2.3.2 Matching algorithms for pairing predicted and experimental pKas

137 Explain why it is necessary due to lacking structural information. Cite recommendations from article such as preserving sequence.

138 Experimental data doesn't inform protonation site and overall charge of species. Experimental data doesn't capture the whole

139 picture. We don't know charge and we don't know tautomers. We don't know the charge state of macrostates, this causes a

140 matching problem

141   Explain Hungarian method for matching experimental and predicted pKas

142   Explain Closest method for matching experimental and predicted pKas

143   Explain microstate based matching.

2.4 Reference calculations

145 Schrodinger Epik Schrodinger Jaguar Chemicalize MoKa

3 Results and Discussion

147 A paragraph to explain the submission methods. Define method categories: DL, LFER, QSPR/ML, QM, QM+LEC, and QM+MM, Blind predictions, Reference calculations, Null model (pKa prospector lookup)

148   Submissions spanning different method categories were made to the SAMPL6 pK_a Challenge: database lookup (DL), linear

149 free energy relationship (LFER), quantitative structure property relationship (QSPR), machine learning (ML), quantum mechanics

150 (QM) models with and without linear empirical correction (LEC), and combined quantum mechanics and molecular mechanics

151 (QM+MM). Unique submission IDs were assigned to each submission. Table 1 matches method names with submission IDs.

152 Unique IDs were also assigned when multiple submissions exists for different submission types of the same method such as

153 microscopic pK_a(type I) and macroscopic pK_a (type III).

3.1 Analysis of macroscopic pK_a predictions (Type III)

155 Refer to SI TABLE: Error statistics for all participants. Refer to SI FIGURE: Error distribution ridge plots for each method (exp-pred

156 macroscopic pKa). Which methods tend to overestimate and which methods tend to undestimate?

157 MI: SI TABLE: Error statistics for all participants

158   Describe number of missing and extra pKa for each method. Report in total for all molecules how many predicted pKas are

159 there and how many experimental pKas. Refer to FIGURE: missing and extra pKa counts.

160 MI: SI TABLE: Missing and extra pKa counts

161   Describe overall performance comparison of different methods, grouped by methods class.

162 Explain rationale behind how we analyze the data and determine success/failure

163 Performance comparison of different methods, grouped by methods class

Table 1. Submission IDs, names, category, and type for all the pKₐ prediction sets. Reference calculations are labeled as *nb###*. The method name column lists the names provided by each participant in the submission file. The "type" column indicates if submission was or a post-deadline reference calculation, denoted by "Blind" or "Reference" respectively. The table is not ordered by performance.

Method Category	Method	Microscopic pK_a (Type I) Submission ID	Macroscopic pK_a (Type III) Submission ID	Submission Type	Ref.
DL	Substructure matches to experimental data in pKa OpenEye pKa Prospector Database v1.0		5nm4j	Null	[2]
DL	OpenEye pKa-Prospector 1.0.0.3 with Analog Search ion identification algorithm		pwn3m	Null	[2]
LFER	ACD/pKa GALAS (ACD/Percepta Kernel v1.6)	v8qph	37xm8	Blind	[3]
LFER	ACD/pKa Classic (ACD/Percepta Kernel, v1.6)		xmyhm	Blind	[4]
LFER	Epik Scan (Schrodinger v2017-4)		nb007	Reference	[5]
LFER	Epik Microscopic (Schrodinger v2017-4)	nb008	nb010	Reference	[5]
QSPR/ML	OpenEye Gaussian Process	6tvf8	hytjn	Blind	[6]
QSPR/ML	OpenEye Gaussian Process Resampled		q3pfp	Blind	[6]
QSPR/ML	S+pKa (ADMET Predictor v8.5, Simulations Plus)	hdiyq	gyuhx	Blind	[7]
QSPR/ML	Chemicalize v18.23 (ChemAxon MarvinSketch v18.23)		nb015	Reference	[8]
QSPR/ML	MoKa v3.1.3	nb016	nb017	Reference	[9, 10]
QM	Adiabatic scheme with single point correction: SMD/M06-2X//6-311++G(d,p)//M06-2X/6-31+G(d) for bases and SMD/M06-2X//6-311++G(d,p)//M06-2X/6-31G(d) for acids + thermal corrections	ko8yx	ryzue	Blind	[11]
QM	Direct scheme with single point correction: SMD/M06-2X//6-311++G(d,p)//M06-2X/6-31+G(d) for bases and SMD/M06-2X//6-311++G(d,p)//M06-2X/6-31G(d) for acids + thermal corrections	w4z0e	xikp8	Blind	[11]
QM	Adiabatic scheme: thermodynamic cycle that uses gas phase optimized structures for gas phase free energy and solution phase geometries for solvent phase free energy. SMD/M06-2X/6-31+G(d) for bases and SMD/M06-2X/6-31G(d) for acids + thermal corrections	wcvnu	5byn6	Blind	[11]
QM	Vertical scheme: thermodynamic cycle that uses only gas phase optimized structures to compute gas hase and solvation free energy. SMD/M06-2X/6-31+G(d) for bases and SMD/M06-2X/6-31G(d) for acids + Thermal corrections	arcko	w4iyd	Blind	[11]
QM	Direct scheme: solution phase free energy is determined by solution phase geometries without thermodynamic cycle SMD/M06-2X/6-31+G(d) for bases and SMD/M06-2X/6-31G(d) for acids + thermal corrections	wexjs	y75vj	Blind	[11]
QM + LEC	Jaguar (Schrodinger v2017-4)	nb011	nb013	Reference	[12]
QM + LEC	CPCM/B3LYP/6–311+G(d,p) and global fitting	y4wws	35bdm	Blind	[13]
QM + LEC	CPCM/B3LYP/6–311+G(d,p) and separate fitting for neutral to negative and for positive to neutral transformations	qsicn	p0jba	Blind	[13]
QM + LEC	EC-RISM/MP2/6-311+G(d,p)-P3NI-q-noThiols-2par	kxztt	ds62k	Blind	[14]
QM + LEC	EC-RISM/MP2/cc-pVTZ-P2-q-noThiols-2par	ftc8w	2ii2g	Blind	[14]
QM + LEC	EC-RISM/MP2/6-311+G(d,p)-P2-phi-all-2par	ktpj5	nb001	Blind*	[14]
QM + LEC	EC-RISM/MP2/6-311+G(d,p)-P2-phi-noThiols-2par	wuuvc	nb002	Blind*	[14]
QM + LEC	EC-RISM/MP2/6-311+G(d,p)-P3NI-phi-all-2par	2umai	nb003	Blind*	[14]
QM + LEC	EC-RISM/MP2/6-311+G(d,p)-P3NI-phi-noThiols-2par	cm2yq	nb004	Blind*	[14]
QM + LEC	EC-RISM/MP2/6-311+G(d,p)-P2-phi-all-1par	z7fhp	nb005	Blind*	[14]
QM + LEC	EC-RISM/MP2/6-311+G(d,p)-P3NI-phi-all-1par	8toyp	nb006	Blind*	[14]
QM + LEC	EC-RISM/MP2/cc-pVTZ-P2-phi-noThiols-2par	epvmk	ttjd0	Blind	[14]
QM + LEC	EC-RISM/MP2/cc-pVTZ-P2-phi-all-2par	xnoe0	mkhqa	Blind	[14]
QM + LEC	EC-RISM/MP2/cc-pVTZ-P3NI-phi-noThiols-2par	4o0ia	mpwiy	Blind	[14]
QM + LEC	EC-RISM/B3LYP/6-311+G(d,p)-P3NI-q-noThiols-2par	nxaaw	ad5pu	Blind	[14]
QM + LEC	EC-RISM/B3LYP/6-311+G(d,p)-P3NI-phi-noThiols-2par	0xi4b	f0gew	Blind	[14]
QM + LEC	EC-RISM/B3LYP/6-311+G(d,p)-P2-phi-noThiols-2par	cywyk	np6b4	Blind	[14]
QM + LEC	PCM/B3LYP/6-311+G(d,p)	gdqeg	yc70m	Blind	[14]
QM + LEC	COSMOtherm_FINE17 (COSMOtherm C30_1701, BP/TZVPD/FINE//BP/TZVP/COSMO)	t8ewk	0hxtm	Blind	[15, 16]
QM + LEC	DSD-BLYP-D3(BJ)/def2-TZVPD//PBEh-3c[DCOSMO-RS] + RRHO(GFN-xTB[GBSA]) + Gsolv(COSMO-RS[TZVPD]) and linear fit		xvxzd	Blind	[17]
QM + LEC	ReSCoSS conformations // DSD-BLYP-D3 reranking // COSMOtherm pKa: DSD-BLYP-D3(BJ)/def2-TZVPD// PBE-D3(BJ)/def2-TZVP/COSMO + RRHO[GFN-xTB + GBSA-water] + Gsolv[COSMO-RS(FINE17/TZVPD)] level and COSMOtherm pKa applied at the single conformer pair level (COSMOthermX17.0.5 release and BP-TZVPD-FINE-C30-1701 parameterization)	eyetm	8xt50	Blind	[17]
QM + LEC	ReSCoSS conformations // COSMOtherm pKa: DSD-BLYP-D3(BJ)/def2-TZVPD// PBE-D3(BJ)/def2-TZVP/COSMO + RRHO[GFN-xTB + GBSA-water] + Gsolv[COSMO-RS(FINE17/TZVPD)] level and COSMOtherm pKa was applied directly on the resulting conformer sets with at least 5% Boltzmann weights for each microspecies (COSMOthermX17.0.5 release and BP-TZVPD-FINE-C30-1701 parameterization)	ccpmw	yqkga	Blind	[17]
QM + MM	M06-2X/6-31G*(for bases) or 6-31+G*(for acids) for gas phase, solvation free energy using TI with explicit solvent and GAFF, solvation free energy of proton -265.6 kcal/mol	0wfzo		Blind	[18]
QM + MM	M06-2X/6-31G*(for bases) or 6-31+G*(for acids) for gas phase, solvation free energy using TI with explicit solvent and GAFF, solvation free energy of proton -271.88 kcal/mol	z3btx		Blind	
QM + MM	M06-2X/6-31G*(for bases) or 6-31+G*(for acids) + thermal state correction for gas phase, solvation free energy using TI with explicit solvent and GAFF, solvation free energy of proton -265.6 kcal/mol	758j8		Blind	
QM + MM	M06-2X/6-31G*(for bases) or 6-31+G*(for acids) + thermal state correction for gas phase, solvation free energy using TI with explicit solvent and GAFF, solvation free energy of proton -271.88 kcal/mol	hgn83		Blind	

* Microscopic pK_a submissions were blind, however, participant requested a correction after blind submission deadline for macroscopic pK_a submissions. Therefore, these were assigned submission IDs in the form of *nb###*.
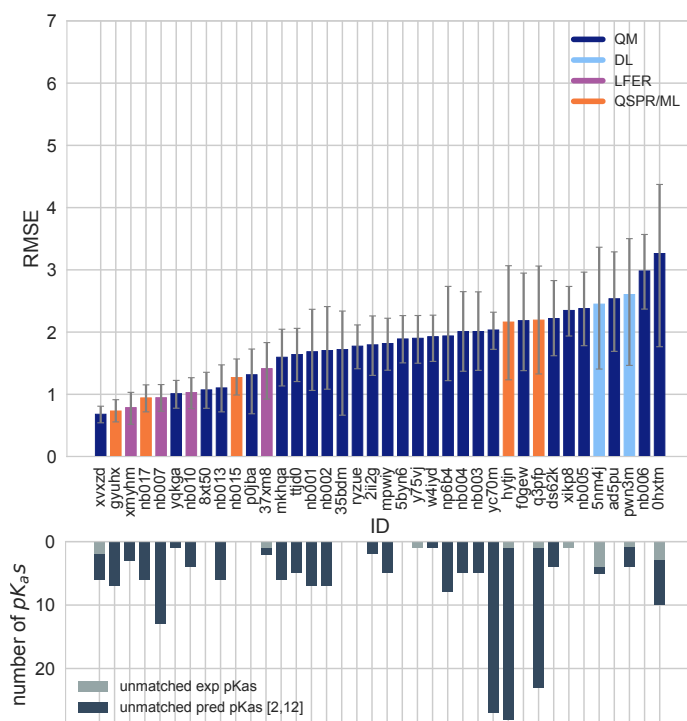
Figure 2. RMSE and unmatched pK_a counts vs. submission ID plots for macroscopic pK_a predictions based on Hungarian matching. Methods are indicated by submission IDs. RMSE is shown with error bars denoting 95% confidence intervals obtained by bootstrapping over challenge molecules. Lower bar plots show the number of unmatched experimental pK_as (light grey, missing predictions) and the number of unmatched pK_a predictions (dark grey, extra predictions) for each method between pH 2 and 12. Submission IDs are summarized in Table 1. Submission IDs of the form *nb###* refer to non-blinded reference methods computed after the blind challenge submission deadline. All others refer to blind, prospective predictions. Submissions are colored by their method categories. Light blue colored database look up methods are utilized as the null prediction method.
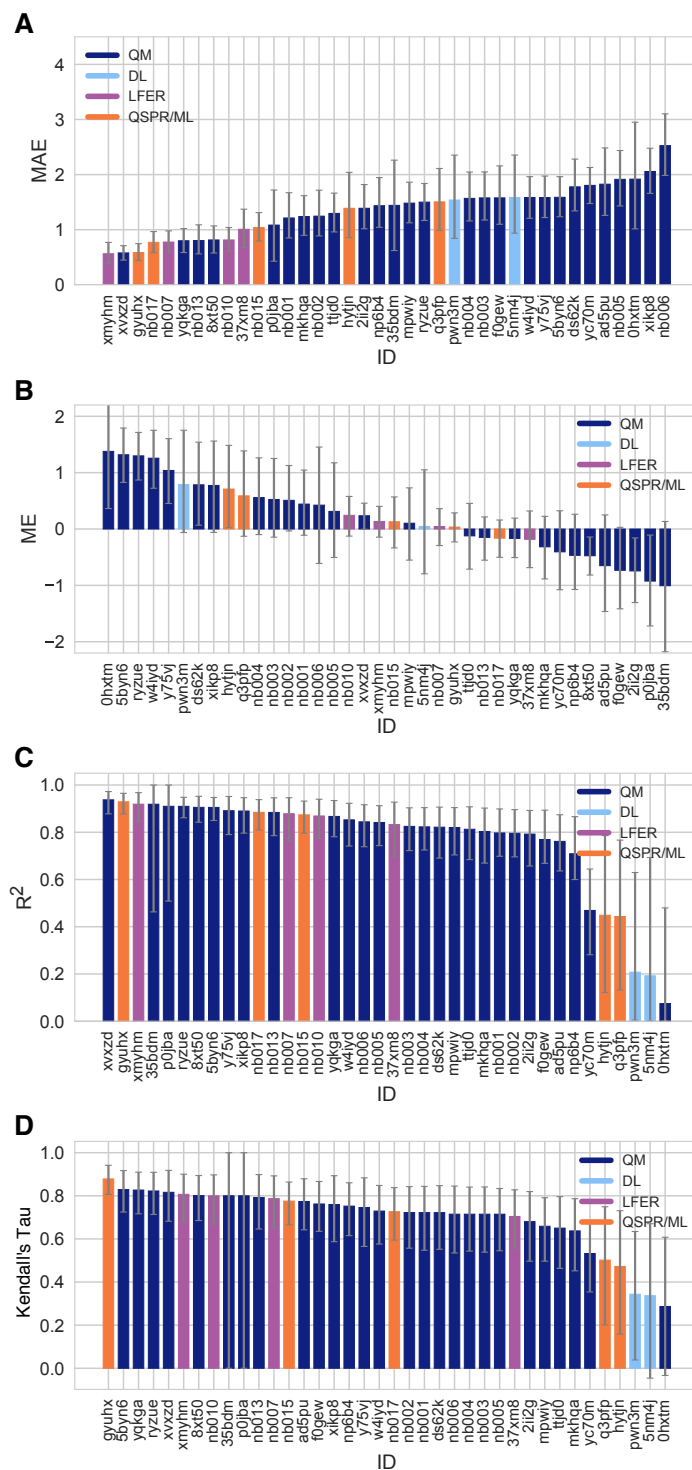
Figure 3. Additional performance statistics for macrocopic pK_a predictions based on Hungarian matching. Methods are indicated by submission IDs. Mean absolute error (MAE), mean error (ME), Pearson's R^2, and Kendall's Rank Correlation Coefficient Tau (τ) are shown, with error bars denoting 95% confidence intervals obtained by bootstrapping over challenge molecules. Refer to Table 1 for submission IDs and method names. Submissions are colored by their method categories. Light blue colored database look up methods are utilized as the null prediction method.

164   Method comparison based on statistical metrics. Explain the numerical matching methods used. Explain rationale behind

165 how we analyze the data and determine success/failure. Method comparison according to different statistics: RMSE, MAE, ME,

166 R2, m, Kendall's tau.

167 ### 3.1.1   Consistently well performing methods for macroscopic pK_a prediction

Table 2. Four consistently well-performing prediction methods for macroscopic pK_a prediction based on consistent ranking within the Top 10 according to various statistical metrics. Submissions were ranked according to RMSE, MAE, R^2, and τ. Consistently well-performing methods were selected as the ones that rank in the Top 10 in each of these statistical metrics. These methods also have less than 2 unmatched experimental pK_as and less than 7 unmatched predicted pK_as according to Hungarian matching. Performance statistics are provided as mean and 95% confidence intervals.

Submission ID	Method Name	RMSE	MAE	R^2	Kendall's Tau (τ)	Unmatched Exp. pK_a Count	Unmatched Pred. pK_a Count [2,12]
xvxzd	Full quantum chemical calculation of free energies and fit to experimental pKa	0.68 [0.54, 0.81]	0.58 [0.45, 0.71]	0.94 [0.88, 0.97]	0.82 [0.68, 0.92]	2	4
gyuhx	S+pKa	0.73 [0.55, 0.91]	0.59 [0.44, 0.74]	0.93 [0.88, 0.96]	0.88 [0.8, 0.94]	0	7
xmyhm	ACD/pKa Classic	0.79 [0.52, 1.03]	0.56 [0.38, 0.77]	0.92 [0.85, 0.97]	0.81 [0.68, 0.9]	0	3
8xt50	ReSCoSS conformations // DSD-BLYP-D3 reranking // COSMOtherm pKa	1.07 [0.78, 1.36]	0.81 [0.58, 1.07]	0.91 [0.84, 0.95]	0.80 [0.68, 0.89]	0	0

168   Check if top few performing methods are consistent between error metrics.

169 ### 3.1.2   Which chemicals are harder to predict?

170 For physical prediction methods sulfur containing heterocycles, amide next to aromatic heterocycles, compounds with iodo and

171 bromo domains have lower pKa prediction accuracy.

172   Prediction performance of individual molecules

173   Which chemical structures make pKa predictions more difficult?

174   SAMPL6 pKa set consisted of only 24 small molecules which limits our ability to do statistical analysis to determine which

175 chemical substructures contribute to greater errors in pKa predictions.

176   Illustration/explanation of effects where microscopic pKas and macroscopic pKas can differ

177   Are there any correlations between molecular descriptors and pKa errors?

178   What can we learn from failures? Which physical effects are driving failures?

179   Does molecular descriptors explain errors/performance ? We looked for correlation with descriptors, and potential expla-

180 nation for errors. Keep spurious correlations in mind if we have many descriptors. No correlation observed. Reference the SI

181 Figure of correlations.

182   Comparison of errors/performance against molecular descriptors. Look for correlation with descriptors, and potential explanation for errors. Keep spurious correlations in mind if we have many descriptors.

183   MI: Figure SI: correlation between prediction error and molecular descriptors

184   Are pKa predictions better in middle region? No correlation between pKa value and error was seen. Reference the SI Figure.

185   Refer to Ridge plots of Delta pKa error to identify compounds that were frequently mispredicted.

186   Compare ME of molecules across methods. Are there molecules often overestimated or underestimated?

187   No correlation of macroscopic pKa number to the errors? But we have low representation of multiprotic compounds

188 ## 3.2   Analysis of microscopic pK_a predictions using microstates determined by NMR (8 molecules)

189 ### 3.2.1   Comparing microscopic pKa predictions directly to macroscopic experimental pKa values with numerical

190   matching leads to underestimation of errors

191 Demonstrate how numerical matching often masks the error Match by Hungarian and calculate accuracy of microstate predic-

192 tion overall. When matched by pKa value, do people come with the same transition pairs?

193   MI: SI FIGURE: [accuracy-of-microstates-based-on-numeric-matching] For most methods the microstate pair of Hungarian predicted pKa does not match experimentally determined microstate pair.
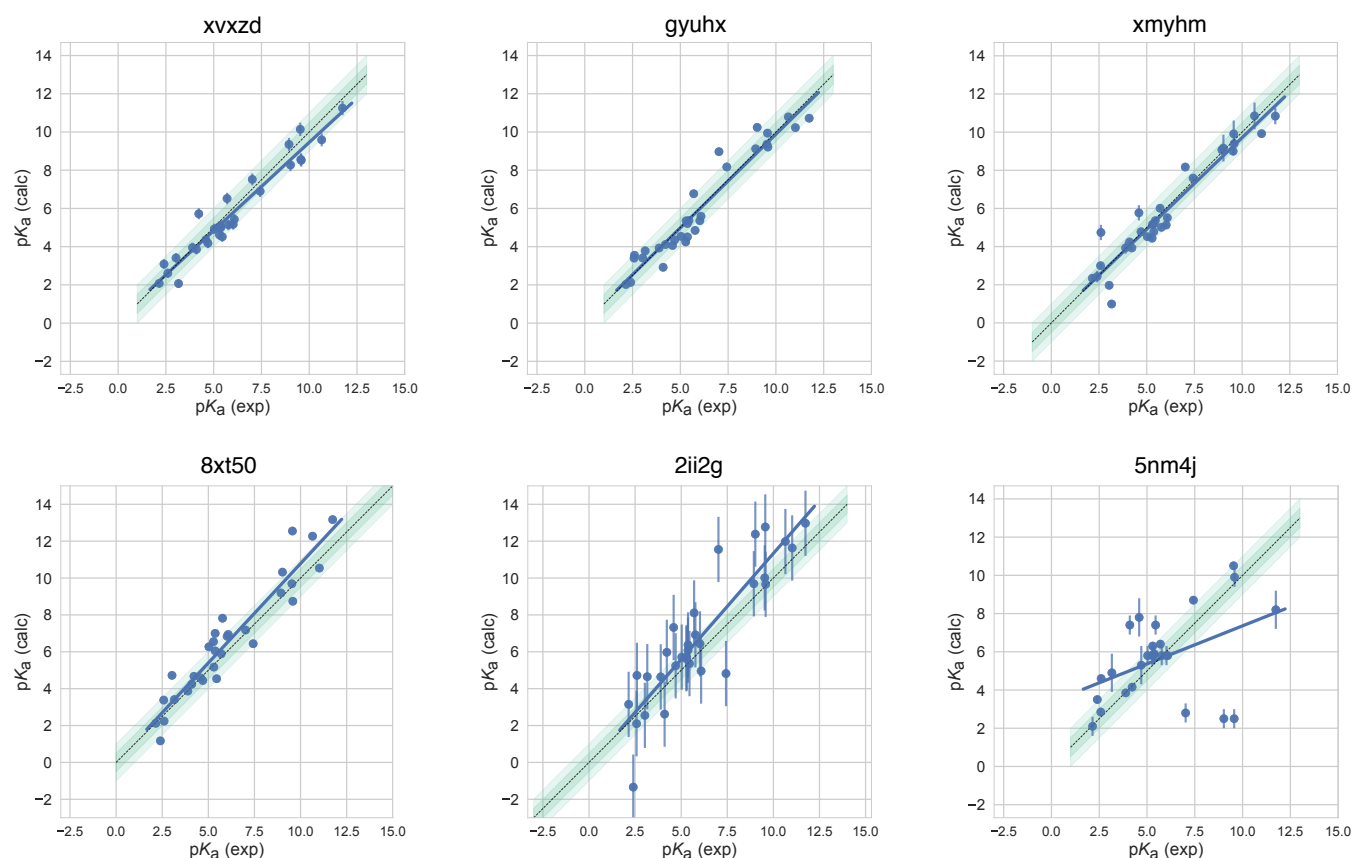
Figure 4. Predicted vs. experimental value correlation plots of 4 consistently well-performing methods, a representative method with average performance (*2ii2g*), and the null method (*5nm4j*). Dark and light green shaded areas indicate 0.5 and 1.0 units of error. Error bars indicate standard error of the mean of predicted and experimental values. Experimental pK_a SEM values are too small to be seen under the data points. EC-RISM/MP2/cc-pVTZ-P2-q-noThiols-2par method (*2ii2g*) was selected as the representative method with average performance because it is the method with the highest RMSE below the median.
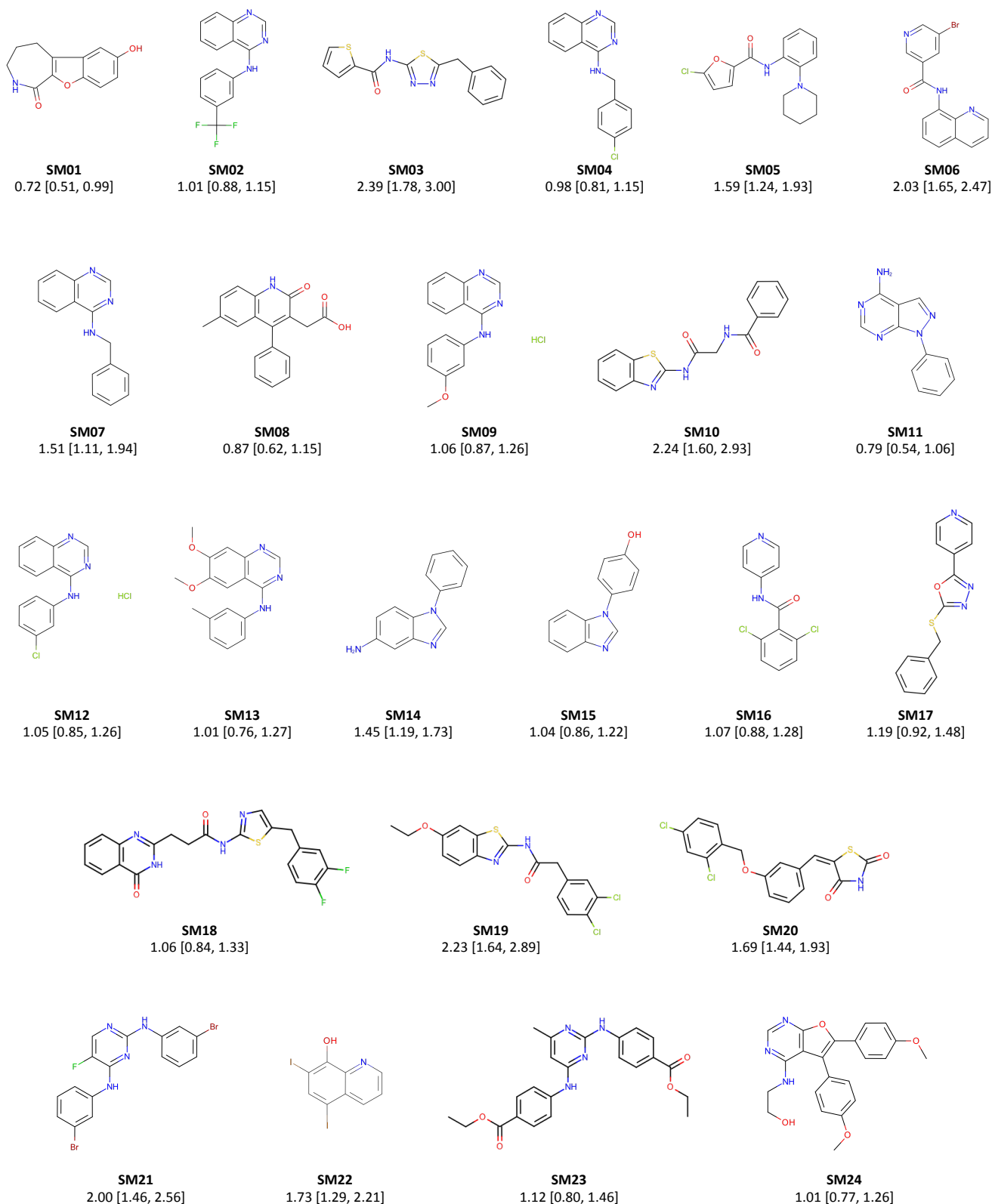
SM01
0.72 [0.51, 0.99]

SM02
1.01 [0.88, 1.15]

SM03
2.39 [1.78, 3.00]

SM04
0.98 [0.81, 1.15]

SM05
1.59 [1.24, 1.93]

SM06
2.03 [1.65, 2.47]

SM07
1.51 [1.11, 1.94]

SM08
0.87 [0.62, 1.15]

SM09
1.06 [0.87, 1.26]

SM10
2.24 [1.60, 2.93]

SM11
0.79 [0.54, 1.06]

SM12
1.05 [0.85, 1.26]

SM13
1.01 [0.76, 1.27]

SM14
1.45 [1.19, 1.73]

SM15
1.04 [0.86, 1.22]

SM16
1.07 [0.88, 1.28]

SM17
1.19 [0.92, 1.48]

SM18
1.06 [0.84, 1.33]

SM19
2.23 [1.64, 2.89]

SM20
1.69 [1.44, 1.93]

SM21
2.00 [1.46, 2.56]

SM22
1.73 [1.29, 2.21]

SM23
1.12 [0.80, 1.46]

SM24
1.01 [0.77, 1.26]

Figure 5. Molecules of SAMPL6 Challenge with MAE calculated for all macroscopic pK_a predictions. MAE calculated considering all prediction methods indicate which molecules had the lowest prediction accuracy in SAMPL6 Challenge. MAE values calculated for each molecule include all the matched pK_a values, which could be more than one per method for multiprotic molecules (SM06, SM14, SM15, SM16, SM18, SM22). Hungarian matching algorithm wasemployed for pairing experimental and predicted pK_a values. MAE values are reported with 95% confidence intervals.
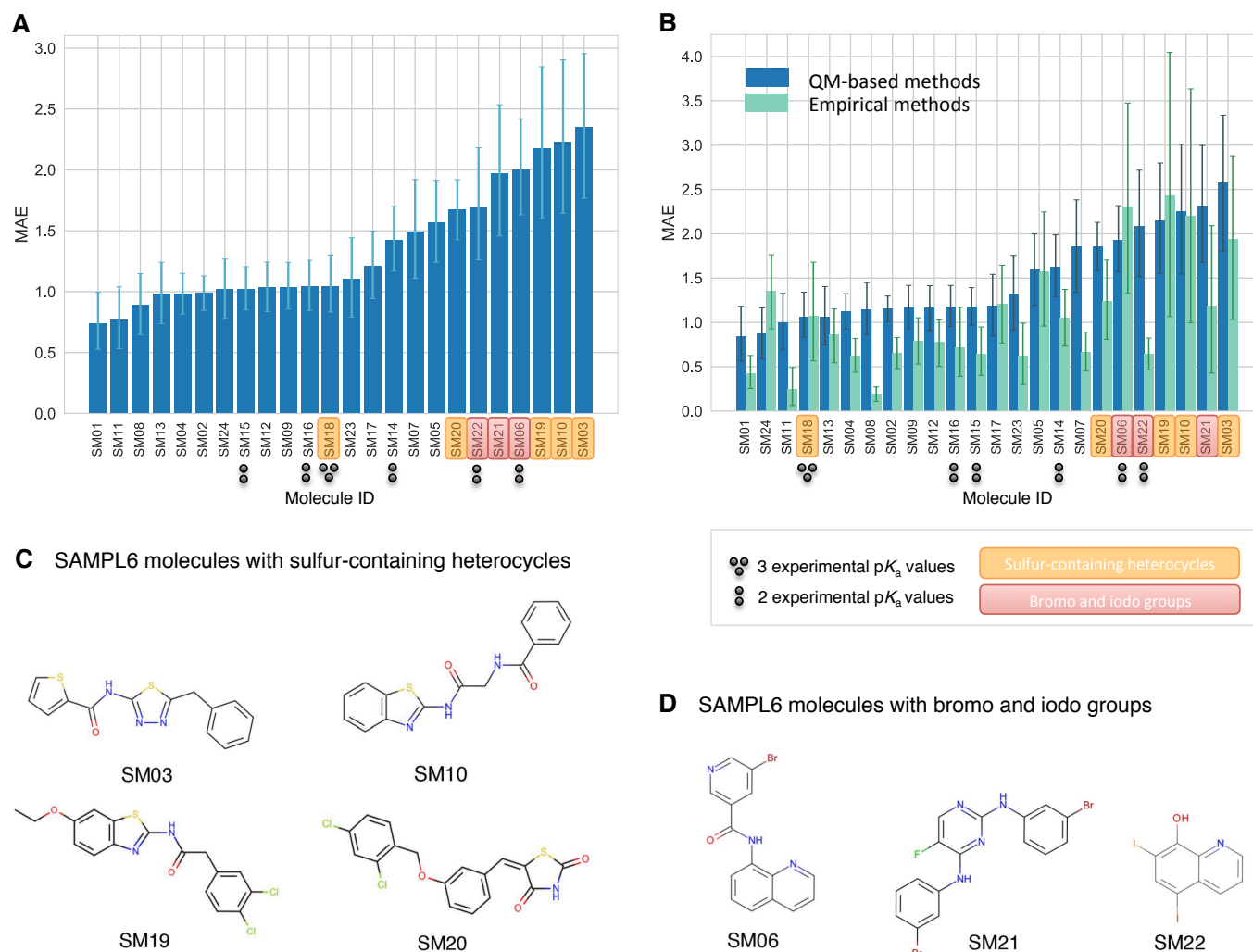
Figure 6. Average prediction accuracy calculated over all prediction methods was lower for molecules with sulfur-containing heterocycles, bromo, and iodo groups. (A) MAE calculated for each molecule as an average of all methods. **(B)** MAE of each molecule broken out by method category. QM-based methods (blue) include QM predictions with or without linear empirical correction. Empirical methods (green) include QSAR, ML, DL, and LFER approaches. **(C)** Depiction of SAMPL6 molecules with sulfur-containing heterocycles. **(D)** Depiction of SAMPL6 molecules with iodo and bromo groups .
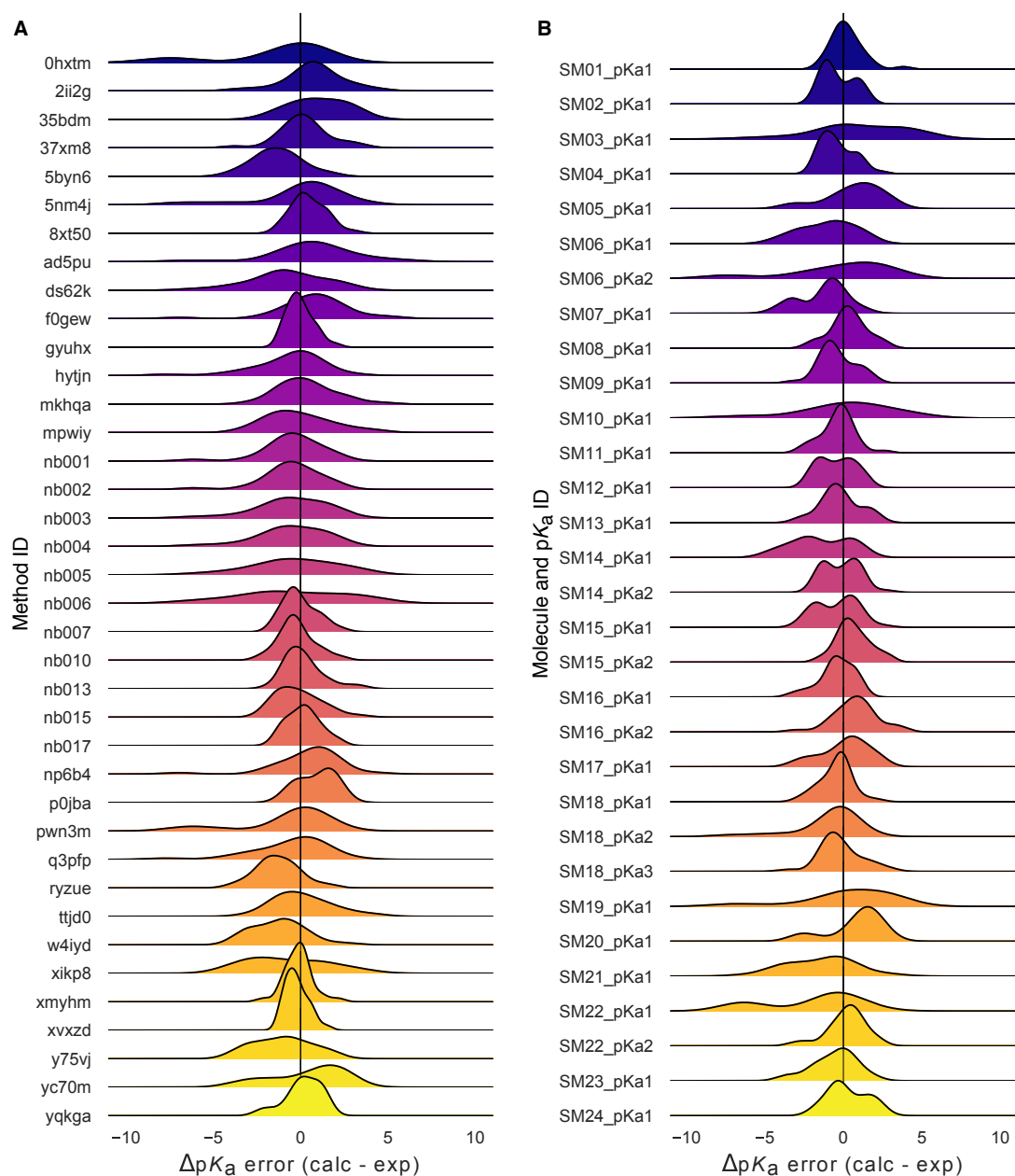
Figure 7. Macroscopic pK_a prediction error distribution plots show how prediction accuracy varies across methods and individual molecules. (A) pK_a prediction error distribution for each submission for all molecules according to Hungarian matching. **(B)** Error distribution for each SAMPL6 molecule for all prediction methods according to Hungarian matching. For multiprotic molecules, pK_a ID numbers (pKa1, pKa2, and pKa3) were assigned in the direction of increasing experimental pK_a value.
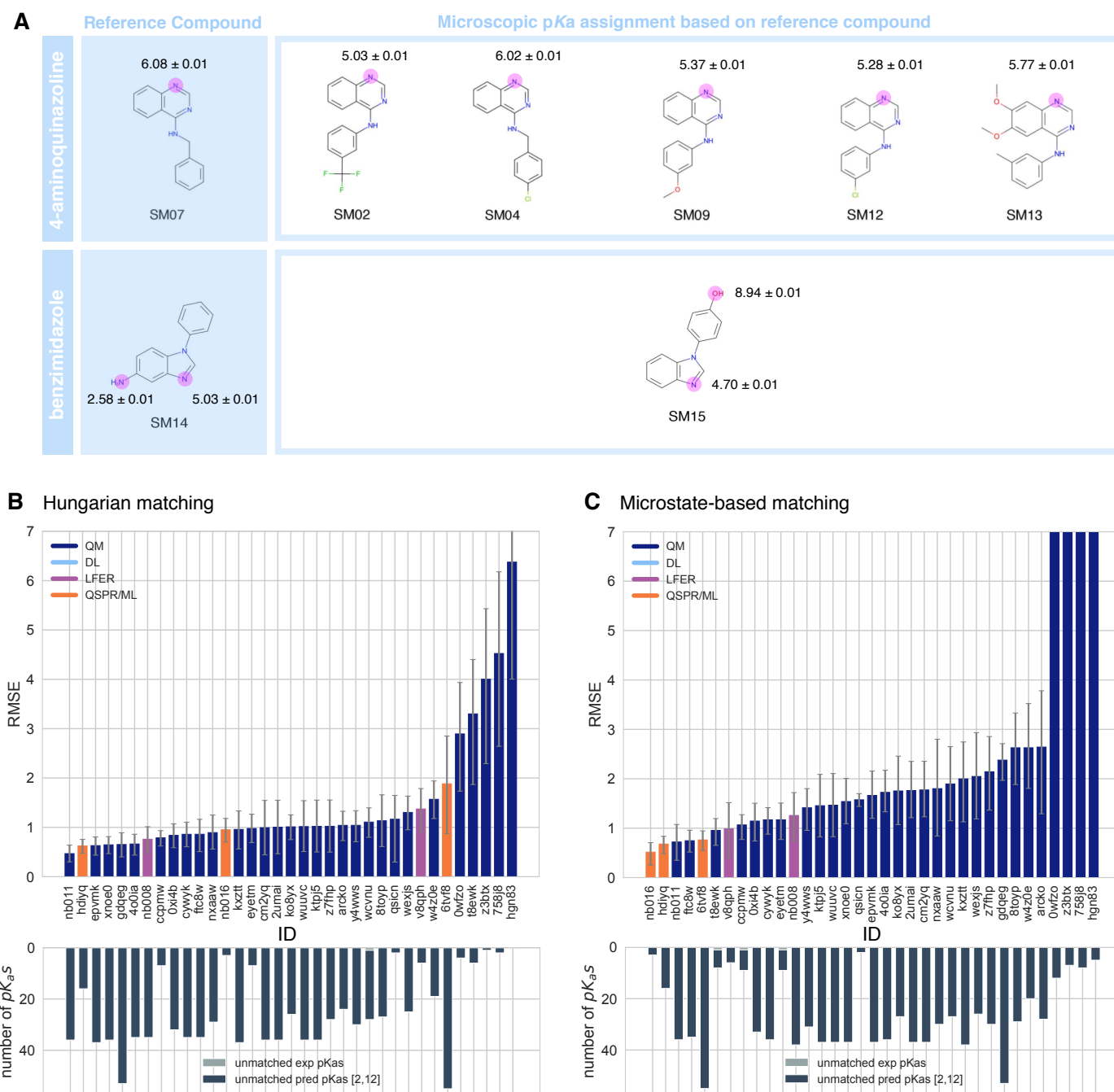
Figure 8. NMR determination of dominant microstates allowed in depth evaluation of microscopic pK_a predictions of 8 compounds.
A Dominant microstate sequence of two compounds (SM07 and SM14) were determined by NMR [1]. Based on these reference compounds dominant microstates of 6 other derivative compounds were infered and experimental pK_a values were assigned to titratable groups with the assumption that only the dominant microstates have significant contributions to the experimentally observed pK_a. **B** RMSE vs. submission ID and unmatched pK_a vs. submission ID plots for the evaluation of microscopic pK_a predictions of 8 molecules by Hungarian matching to experimental macroscopic pK_as. **C** RMSE vs. submission ID and unmatched pK_a vs. submission ID plots showing the evaluation of microscopic pK_a predictions of 8 molecules by microstate-based matching between predicted microscopic pK_as and experimental macroscopic pK_a values. Submissions *0wfzo, z3btx, 758j8,* and *hgn83* have RMSE values bigger than 10 pK_a units which are beyond the y-axis limits of subplot **C** and **B**. RMSE is shown with error bars denoting 95% confidence intervals obtained by bootstrapping over challenge molecules. Lower bar plots show the number of unmatched experimental pK_as (light grey, missing predictions) and the number of unmatched pK_a predictions (dark grey, extra predictions) for each method between pH 2 and 12. Submission IDs are summarized in Table 1.

Discussion of matching experimental and predicted values

Compare experimental data to microscopic pKa predictions, assuming experimental pKas are titrations of distinguishable sides and therefore equal to microscopic pKas. Molecules with only 1 pKa or well separated multiple pKas (more than 3 pKa units apart) SM14 and SM18 were excluded from this analysis, since their experimental pKa values don't satisfy these criteria.

Errors computed by microstate-based matching are larger compared to numerical matching algorithms. Microscopic pKa analysis with numerical matching algorithms may mask errors due to higher number of guesses made.

Conclusions will only be about 4-aminoquinazoline series and benzimidazole (8 molecules, 10 pKas) Refer to SI figure of dominant microstates.

Choosing molecules with right protonation state is important. Do people predict the correct sequence of dominant microstates? " Even if your pKa prediction is correct, protonation state prediction can be wrong." Analyze which state has lowest free energy for each charge group (The sequence of "experimentally visible states")

3.2.2   Accuracy of predicted pKa values when microstate matching is used

Assessment of individual methods by each of our analysis methods

Performance comparison of different methods, grouped by methods class

Comment on the ranking of microscopic pKa prediction error statistsics for all participants (8 mol, microstate match). Refer to Fig. 9

3.2.3   Dominant microstate prediction accuracy of methods

Calculate relative free energy of microstates to determine dominant microstate of each charge Compare predicted and experimental dominant microstates and calculate accuracy of each method

What percent of the time predictions capture the dominant protonation state correctly? Match by microstate and calculate RMSE and MAE. If you know the microstates, can you predict the value of the pKa right?

Does top 3 methods predict the same dominant microstate sequence? How differently do different methods predict microscopic transitions? (method vs method correlation plot to see if methods predict the same microstate pairs or not)

3.2.4   Which molecules caused lower dominant microstate prediction accuracy?

Which molecule has more errors in predicting the major microstates?

Comment on consensus prediction accuracy. Comparison of predicted microstates using consensus set of transitions of high accuracy prediction methods

3.3   Analyzing microscopic pKa prediction from the perspective of thermodynamics

Explain linearity relative free energy of protonation states with respect to pH. Free energy perspective simplifies data capturing and analysis. Reference Marilyn's paper.

Thermodynamic cycle closure checking allows evaluation of microsopic pKas without experimental data. Checking for thermodynamic consistency

3.3.1   Cycle closure error

Marilyn observed very good cycle closure results and very bad one that are up to 10 kcal/mol

She suggesting checking the cycle with maximum cycle closure error for each method and reporting that for each method. An historgam of max cycle closure error will help us bin these results into 3 categoris: 1. good agreement 2. moderate 3. severe

"We think thermodyamic cycles of protonation states need to be closed" Message: Methods need to checked for cycle closure errors. There can be information there that can be used to correct pKa predictions. When cycles are not closed it may be used as an indicator of prediction uncertainty.
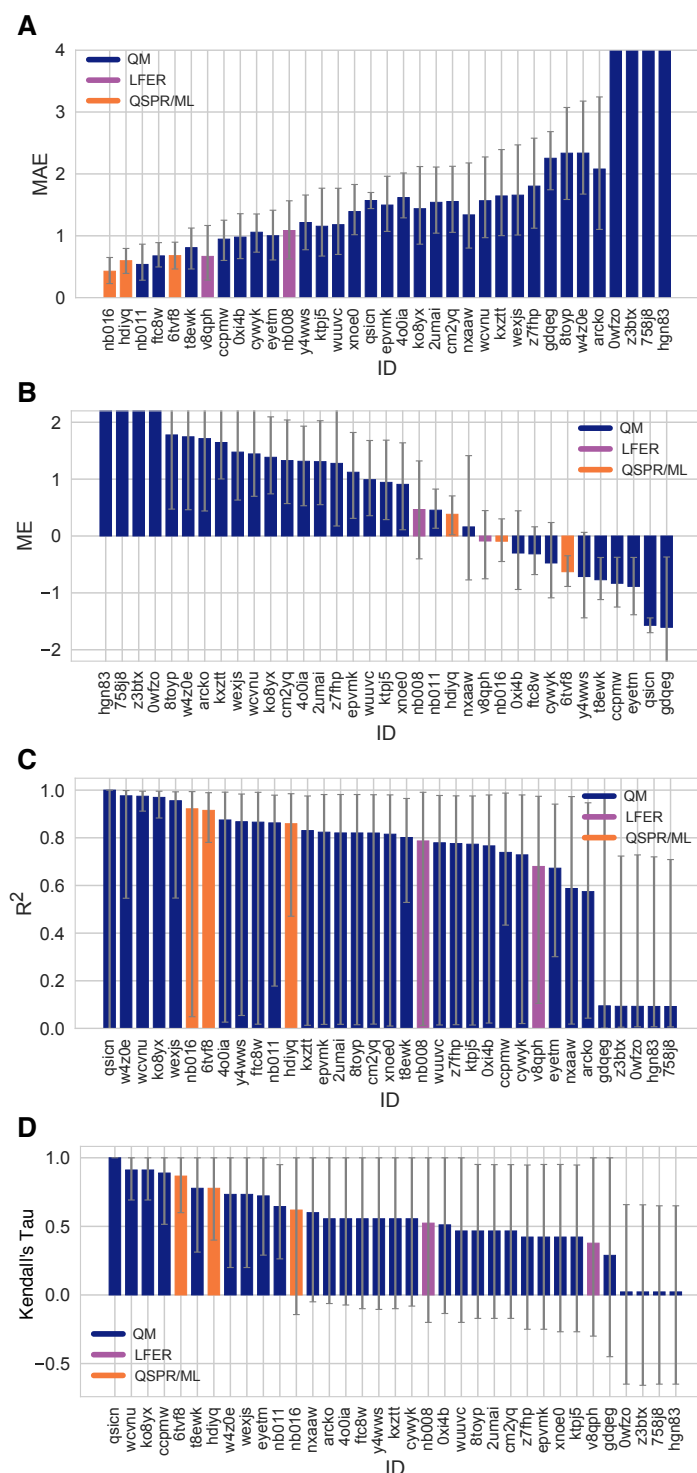
Figure 9. Additional performance statistics for microscopic pK_a predictions for 8 molecules with experimentally determined dominant microstates. Microstate-based matching was performed between experimental pK_a values and predicted microscopic pK_as. Mean absolute error (MAE), mean error (ME), Pearson's R^2, and Kendall's Rank Correlation Coefficient Tau (τ) are shown, with error bars denoting 95% confidence intervals obtained by bootstrapping over challenge molecules. Methods are indicated by submission IDs. Submissions are colored by their method categories. Refer to Table 1 for submission IDs and method names. Submissions *0wfzo, z3btx, 758j8*, and *hgn83* have MAE and ME values bigger than 10 pK_a units which are beyond the y-axis limits of subplots **A** and **B**. A large number and wide variety of methods have a statistically indistinguishable performance based on correlation based statistic (**C** and **D**), in part because of the relatively small dynamic range the small size of the set of 8 molecules.
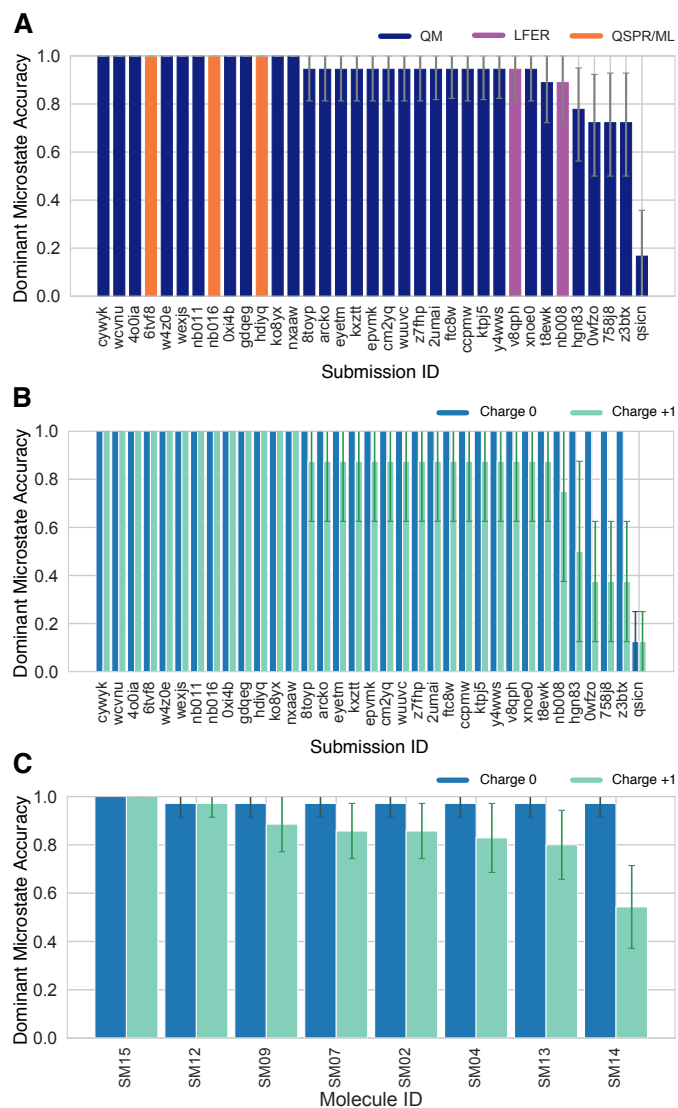
Figure 10. Some methods predicted the sequence of dominant tautomers inaccurately. Prediction accuracy of dominant microstate of each charged state was calculated using the dominant microstate sequence determined by NMR for 8 molecules as reference. **(A)** Dominant microstate accuracy vs. submission ID plot was calculated considering all the dominant microstates seen in the 8 molecule experimental microstate dataset. **(B)** Dominant microstate accuracy vs. submission ID plot was generating considering only the dominant microstates of charge 0 and +1 seen in the 8 molecule experimental microstate dataset. Accuracy of each molecule is broken out by total charge of the microstate. **(C)** Dominant microstate prediction accuracy calculated for each molecule averaged over all methods. In **(B)** and **(C)**, the accuracy of predicting the dominant neutral tautomer is showed in blue and the accuracy of predicting the dominant +1 charged tautomer is showed in green. Error bars denoting 95% confidence intervals obtained by bootstrapping.

3.4 How would pKa errors affect protein-ligand binding affinity predictions?

> Illustrate the ways in which the pKa errors can influence prediction errors for binding affinities

> How do accuracy limitations in small molecule pKa prediction translate into modeling errors in ligand affinity prediction?

> MI: FIGURE: a diagram illustrating the ways in which the pKa errors can influence prediction errors for binding affinities (A) When minor aqueous protonation state binds (B) When multiple protonation states can bind the complex

3.5 Lessons learned from SAMPL6 pKa Challenge

> Do any methods predict within experimental accuracy (how is the field doing overall)?

> Common challenging factors for accurate pKa predictions. Tautomers, Heterocycles etc.

Overall results: Do any methods predict within experimental accuracy (how is the field doing overall)? Common challenging factors for accurate pKa predictions. Tautomers, Heterocycles etc.

Discussion of matching problem betwene experimental and predicted values. Difficulty of assessing predicted pKas using experimental data: matching problem Explain rationale behind how we analyze the data and determine success/failure.

Conclusion about prediction performance of individual molecules: SAMPL6 pKa set consisted of only 24 small molecules which limits our ability to do statistical analysis to determine which chemical substructures contribute to greater errors in pKa predictions. Which chemical structures make pKa predictions more difficult?

What can we learn from failures? Which physical effects are driving failures? Cycle closure errors

3.6 Suggestions for future challenges

> Discuss what can be done to further improve future challenges

How can we maximize what we learn? What should we have people predict? How should we select compounds / measure pKas?

> Suggestions about challenge construction

Enumeration of protonation states before predictions (which states does one need to consider?)

> Suggestions about challenge analysis

NMR experimental techniques could be used to validate microstate information in future challenges

Reporting microscopic pKa predictions with charges, microstate free energies is betetr Experimental dataset with microstate infromation is more helpful.

What can be done to further improve future challenges How can we maximize what we learn? What should we have people predict? How should we select compounds / measure pKas? NMR experimental techniques could be used to validate microstate information in future challenges

Suggestions about challenge construction Enumeration of protonation states before predictions (which states does one need to consider?) Suggestions about challenge analysis

4 Conclusion

5 Code and data availability

- SAMPL6 pK_a challenge instructions, submissions, experimental data and analysis is available at
  https://github.com/samplchallenges/SAMPL6

6 Overview of supplementary information

Organized in SI document:

- TABLE SI 1: SMILES and InChI identifiers of SAMPL6 pK_a Challenge molecules.

Extra files:

- SAMPL6-pKa-chemical-identifiers-table.csv

7 Author Contributions

Conceptualization, MI, JDC, CB, DLM ; Methodology, MI, JDC ; Software, MI, AR, ASR ; Formal Analysis, MI, ASR, AR ; Investigation, MI ; Resources, JDC; Data Curation, MI ; Writing-Original Draft, MI, JDC; Writing - Review and Editing, MI, ASR, AR, CB, DLM, JDC; Visualization, MI, AR ; Supervision, JDC, DLM, CB, ASR ; Project Administration, MI ; Funding Acquisition, JDC, DLM.

8 Acknowledgments

9 Disclosures

JDC is a member of the Scientific Advisory Board for Schrödinger, LLC. DLM is a member of the Scientific Advisory Board of OpenEye Scientific Software.
   Table ref: [3, 4, 7, 8, 10] trial: [], +, -, *, #, \m

References

[1] **Işık M**, Levorse D, Rustenburg AS, Ndukwe IE, Wang H, Wang X, Reibarkh M, Martin GE, Makarov AA, Mobley DL, Rhodes T, Chodera JD. pKa Measurements for the SAMPL6 Prediction Challenge for a Set of Kinase Inhibitor-like Fragments. Journal of Computer-Aided Molecular Design. 2018 Oct; 32(10):1117–1138. doi: 10.1007/s10822-018-0168-0.

[2] OpenEye pKa Prospector;. OpenEye Scientific Software, Santa Fe, NM. Accessed on Jan 23, 2018. https://www.eyesopen.com/pka-prospector.

[3] ACD/pKa GALAS (ACD/Percepta Kernel v1.6);. Advanced Chemistry Development, Inc., Toronto, ON, Canada, 2018. https://www.acdlabs.com/products/percepta/predictors/pKa/.

[4] ACD/pKa Classic (ACD/Percepta Kernel v1.6);. Advanced Chemistry Development, Inc., Toronto, ON, Canada, 2018. https://www.acdlabs.com/products/percepta/predictors/pKa/.

[5] **Shelley JC**, Cholleti A, Frye LL, Greenwood JR, Timlin MR, Uchimaya M. Epik: A Software Program for pK a Prediction and Protonation State Generation for Drug-like Molecules. Journal of Computer-Aided Molecular Design. 2007 Dec; 21(12):681–691. doi: 10.1007/s10822-007-9133-z.

[6] **Bannan CC**, Mobley DL, Skillman AG. SAMPL6 Challenge Results from $$pK_a$$ Predictions Based on a General Gaussian Process Model. Journal of Computer-Aided Molecular Design. 2018 Oct; 32(10):1165–1177. doi: 10.1007/s10822-018-0169-z.

[7] Simulations Plus ADMET Predictor v8.5;. Simulations Plus, Lancaster, CA, 2018. https://www.simulations-plus.com/software/admetpredictor/physicochemical-biopharmaceutical/.

[8] Chemicalize v18.23 (ChemAxon MarvinSketch v18.23);. ChemAxon, Budapest, Hungary, 2018. https://docs.chemaxon.com/display/docs/pKa+Plugin.

[9] **Milletti F**, Storchi L, Sforna G, Cruciani G. New and Original p K_a Prediction Method Using Grid Molecular Interaction Fields. Journal of Chemical Information and Modeling. 2007 Nov; 47(6):2172–2181. doi: 10.1021/ci700018y.

[10] MoKa;. Molecular Discovery, Hertfordshire, UK, 2018. https://www.moldiscovery.com/software/moka/.

[11] **Zeng Q**, Jones MR, Brooks BR. Absolute and Relative pKa Predictions via a DFT Approach Applied to the SAMPL6 Blind Challenge. Journal of Computer-Aided Molecular Design. 2018 Oct; 32(10):1179–1189. doi: 10.1007/s10822-018-0150-x.

[12] **Bochevarov AD**, Harder E, Hughes TF, Greenwood JR, Braden DA, Philipp DM, Rinaldo D, Halls MD, Zhang J, Friesner RA. Jaguar: A High-Performance Quantum Chemistry Software Program with Strengths in Life and Materials Sciences. International Journal of Quantum Chemistry. 2013 Sep; 113(18):2110–2142. doi: 10.1002/qua.24481.

[13] **Selwa E**, Kenney IM, Beckstein O, Iorga BI. SAMPL6: Calculation of Macroscopic pKa Values from Ab Initio Quantum Mechanical Free Energies. Journal of Computer-Aided Molecular Design. 2018 Oct; 32(10):1203–1216. doi: 10.1007/s10822-018-0138-6.

[14] **Tielker N**, Eberlein L, Güssregen S, Kast SM. The SAMPL6 Challenge on Predicting Aqueous pKa Values from EC-RISM Theory. Journal of Computer-Aided Molecular Design. 2018 Oct; 32(10):1151–1163. doi: 10.1007/s10822-018-0140-z.

[15] **Klamt A**, Eckert F, Diedenhofen M, Beck ME. First Principles Calculations of Aqueous pK_a Values for Organic and Inorganic Acids Using COSMO-RS Reveal an Inconsistency in the Slope of the pK_a Scale. The Journal of Physical Chemistry A. 2003 Nov; 107(44):9380–9386. doi: 10.1021/jp034688o.

[16] **Eckert F**, Klamt A. Accurate Prediction of Basicity in Aqueous Solution with COSMO-RS. Journal of Computational Chemistry. 2006 Jan; 27(1):11–19. doi: 10.1002/jcc.20309.

[17] **Pracht P**, Wilcken R, Udvarhelyi A, Rodde S, Grimme S. High Accuracy Quantum-Chemistry-Based Calculation and Blind Prediction of Macroscopic pKa Values in the Context of the SAMPL6 Challenge. Journal of Computer-Aided Molecular Design. 2018 Oct; 32(10):1139–1149. doi: 10.1007/s10822-018-0145-7.

[18] **Prasad S**, Huang J, Zeng Q, Brooks BR. An Explicit-Solvent Hybrid QM and MM Approach for Predicting pKa of Small Molecules in SAMPL6 Challenge. Journal of Computer-Aided Molecular Design. 2018 Oct; 32(10):1191–1201. doi: 10.1007/s10822-018-0167-1.

10 Supplementary Information

MI: Figure [typeIII-error-dist-by-method] Distribution of prediction errors for each method in SAMPL6 Challenge. Analyses was performed based on Hungarian matching algorithm. Y-axis labels indicate submission IDs of each method.

MI: [pKa-error-vs-pKa-value]. Error in pKa predictions does not correlate with the true value of pKa. Left figure was constructed using closest match between experimental and predicted pKas. Y-axis is absolute residuals of the pKa prediction.

MI: FIGURE [desc-vs-MAE-correlation]. There is no clear correlation between molecular descriptors and mean absolute error for each molecule when calculated for all methods.

MI: SI Table: Type I collection

MI: SI Table: Type III collection

MI: SI Figure: type I correlation plots of each method

MI: SI Figure: type III correlation plots of each method

MI: TABLE: Statistics based on hungarian matching

MI: TABLE: Statistics based on microstate matching

MI: TABLE: NMR determined microstates of 8 molecules

Table S1. SMILES and InChI identifiers of SAMPL6 pK_a Challenge molecules. A CSV version of this table can be found in *SAMPL6-supplementary-documents.tar.gz*.

SAMPL6 Molecule ID	Isomeric SMILES	InChI
SM01	c1cc2c(cc1O)c3c(o2)C(=O)NCCC3	InChI=1S/C12H11NO3/c14-7-3-4-10-9(6-7)8-2-1-5-13-12(15)11(8)16-10/h3-4,6,14H,1-2,5H2,(H,13,15)
SM02	c1ccc2c(c1)c(ncn2)Nc3cccc(c3)C(F)(F)F	InChI=1S/C15H10F3N3/c16-15(17,18)10-4-3-5-11(8-10)21-14-12-6-1-2-7-13(12)19-9-20-14/h1-9H,(H,19,20,21)
SM03	c1ccc(cc1)Cc2nnc(s2)NC(=O)c3cccs3	InChI=1S/C14H11N3OS2/c18-13(11-7-4-8-19-11)15-14-17-16-12(20-14)9-10-5-2-1-3-6-10/h1-8H,9H2,(H,15,17,18)
SM04	c1ccc2c(c1)c(ncn2)NCc3ccc(cc3)Cl	InChI=1S/C15H12ClN3/c16-12-7-5-11(6-8-12)9-17-15-13-3-1-2-4-14(13)18-10-19-15/h1-8,10H,9H2,(H,17,18,19)
SM05	c1ccc(c(c1)NC(=O)c2ccc(o2)Cl)N3CCCCC3	InChI=1S/C16H17ClN2O2/c17-15-9-8-14(21-15)16(20)18-12-6-2-3-7-13(12)19-10-4-1-5-11-19/h2-3,6-9H,1,4-5,10-11H2,(H,18,20)
SM06	c1cc2cccnc2c(c1)NC(=O)c3cc(cnc3)Br	InChI=1S/C15H10BrN3O/c16-12-7-11(8-17-9-12)15(20)19-13-5-1-3-10-4-2-6-18-14(10)13/h1-9H,(H,19,20)
SM07	c1ccc(cc1)CNc2c3ccccc3ncn2	InChI=1S/C15H13N3/c1-2-6-12(7-3-1)10-16-15-13-8-4-5-9-14(13)17-11-18-15/h1-9,11H,10H2,(H,16,17,18)
SM08	Cc1ccc2c(c1)c(c(c(=O)[nH]2)CC(=O)O)c3ccccc3	InChI=1S/C18H15NO3/c1-11-7-8-15-13(9-11)17(12-5-3-2-4-6-12)14(10-16(20)21)18(22)19-15/h2-9H,10H2,1H3,(H,19,22)(H,20,21)
SM09	COc1cccc(c1)Nc2c3ccccc3ncn2.Cl	InChI=1S/C15H13N3O.ClH/c1-19-12-6-4-5-11(9-12)18-15-13-7-2-3-8-14(13)16-10-17-15;/h2-10H,1H3,(H,16,17,18);1H
SM10	c1ccc(cc1)C(=O)NCC(=O)Nc2nc3ccccc3s2	InChI=1S/C16H13N3O2S/c20-14(10-17-15(21)11-6-2-1-3-7-11)19-16-18-12-8-4-5-9-13(12)22-16/h1-9H,10H2,(H,17,21)(H,18,19,20)
SM11	c1ccc(cc1)n2c3c(cn2)c(ncn3)N	InChI=1S/C11H9N5/c12-10-9-6-15-16(11(9)14-7-13-10)8-4-2-1-3-5-8/h1-7H,(H2,12,13,14)
SM12	c1ccc2c(c1)c(ncn2)Nc3cccc(c3)Cl.Cl	InChI=1S/C14H10ClN3.ClH/c15-10-4-3-5-11(8-10)18-14-12-6-1-2-7-13(12)16-9-17-14;/h1-9H,(H,16,17,18);1H
SM13	Cc1cccc(c1)Nc2c3cc(c(c3ncn2)OC)OC	InChI=1S/C17H17N3O2/c1-11-5-4-6-12(7-11)20-17-13-8-15(21-2)16(22-3)9-14(13)18-10-19-17/h4-10H,1-3H3,(H,18,19,20)
SM14	c1ccc(cc1)n2ncnc3c2ccc(c3)N	InChI=1S/C13H11N3/c14-10-6-7-13-12(8-10)15-9-16(13)11-4-2-1-3-5-11/h1-9H,14H2
SM15	c1ccc2c(c1)ncn2c3ccc(cc3)O	InChI=1S/C13H10N2O/c16-11-7-5-10(6-8-11)15-9-14-12-3-1-2-4-13(12)15/h1-9,16H
SM16	c1cc(c(c(c1)Cl)C(=O)Nc2ccncc2)Cl	InChI=1S/C12H8Cl2N2O/c13-9-2-1-3-10(14)11(9)12(17)16-8-4-6-15-7-5-8/h1-7H,(H,15,16,17)
SM17	c1ccc(cc1)CSc2nnc(o2)c3ccncc3	InChI=1S/C14H11N3OS/c1-2-4-11(5-3-1)10-19-14-17-16-13(18-14)12-6-8-15-9-7-12/h1-9H,10H2
SM18	c1ccc2c(c1)c(=O)[nH]c(n2)CCC(=O)Nc3ncc(s3)Cc4ccc(c(c4)F)F	InChI=1S/C21H16F2N4O2S/c22-15-6-5-12(10-16(15)23)9-13-11-24-21(30-13)27-19(28)8-7-18-25-17-4-2-1-3-14(17)20(29)26-18/h1-6,10-11H,7-9H2,(H,24,27,28)(H,25,26,29)
SM19	CCOc1ccc2c(c1)sc(n2)NC(=O)Cc3ccc(c(c3)Cl)Cl	InChI=1S/C17H14Cl2N2O2S/c1-2-23-11-4-6-14-15(9-11)24-17(20-14)21-16(22)8-10-3-5-12(18)13(19)7-10/h3-7,9H,2,8H2,1H3,(H,20,21,22)
SM20	c1cc(cc(c1)OCc2ccc(cc2Cl)Cl)/C=C/3\C(=O)NC(=O)S3	InChI=1S/C17H11ClNO3S/c18-12-5-4-11(14(19)8-12)9-23-13-3-1-2-10(6-13)7-15-16(21)20-17(22)24-15/h1-8H,9H2,(H,20,21,22)/b15-7+
SM21	c1cc(cc(c1)Br)Nc2c(cnc(n2)Nc3cccc(c3)Br)F	InChI=1S/C16H11Br2FN4/c17-10-3-1-5-12(7-10)21-15-14(19)9-20-16(23-15)22-13-6-2-4-11(18)8-13/h1-9H,(H2,20,21,22,23)
SM22	c1cc2c(cc(c(c2nc1)O)I)I	InChI=1S/C9H5I2NO/c10-6-4-7(11)9(13)8-5(6)2-1-3-12-8/h1-4,13H
SM23	CCOC(=O)c1ccc(c1)Nc2cc(nc(n2)Nc3ccc(cc3)C(=O)OCC)C	InChI=1S/C23H24N4O4/c1-4-30-21(28)16-6-10-18(11-7-16)25-20-14-15(3)24-23(27-20)26-19-12-8-17(9-13-19)22(29)31-5-2/h6-14H,4-5H2,1-3H3,(H2,24,25,26,27)
SM24	COc1ccc(cc1)c2c3c(ncnc3oc2c4ccc(cc4)OC)NCCO	InChI=1S/C22H21N3O4/c1-27-16-7-3-14(4-8-16)18-19-21(23-11-12-26)24-13-25-22(19)29-20(18)15-5-9-17(28-2)10-6-15/h3-10,13,26H,11-12H2,1-2H3,(H,23,24,25)